Neutral sphingomyelinase-induced ceramide triggers germinal vesicle breakdown and oxidant-dependent apoptosis in *Xenopus laevis* oocytes

Olga Coll, Albert Morales, José C. Fernández-Checa,[1,2] **and Carmen Garcia-Ruiz**[1,2]

Liver Unit and Centro de Investigaciones Biomédicas Esther Koplowitz, Institut de Malalties Digestives i Metaboliques, Hospital Clínic i Provincial and Centro de Investigación Biomédica en Red de Enfermedades Hepaticas y Digestivas, Instituto Investigaciones Biomédicas August Pi i Sunyer and Department of Cell Death and Proliferation, Instituto Investigaciones Biomédicas Barcelona, Consejo Superior de Investigaciones Científicas, 08036-Barcelona, Spain

Abstract Ceramide regulates many cellular processes, including cell growth, differentiation, and apoptosis. Although the effects of exogenous bacterial neutral sphingomyelinase (SMase) in *Xenopus laevis* oocytes have been investigated, its microinjection into oocytes has not been reported previously. Thus, we compared the incubation versus microinjection of the neutral *Bacillus cereus* sphingomyelinase (bSMase) to examine whether the topology of ceramide generation determines its effects on the fate of oocytes. In agreement with previous findings, incubation of mature stage VI oocytes with bSMase increased ceramide levels in oocyte extracts over time, causing the germinal vesicle breakdown indicative of maturation, without evidence of cytotoxicity. In contrast, bSMase microinjection, which increased ceramide levels in a time- and dose-dependent manner, resulted in oocyte apoptosis characterized by reactive oxygen species (ROS) generation, reduced glutathione (GSH) depletion in cytosol and mitochondria, release of cytochrome c and Smac/Diablo from mitochondria, and caspase-3 activation. Microinjection of acidic SMase from human placenta recapitulated the apoptotic effects of bSMase microinjection. Preincubation of oocytes with GSH-ethyl ester before bSMase microinjection prevented ROS generation and mitochondrial downstream events, thus protecting oocytes from bSMase-induced death.🔓 These findings show a divergent action of bSMase-induced ceramide on oocyte maturation or apoptosis depending on the intracellular site where ceramide is generated.—Coll, O., A. Morales, J. C. Fernández-Checa, and C. Garcia-Ruiz. **Neutral sphingomyelinase-induced ceramide triggers germinal vesicle breakdown and oxidant-dependent apoptosis in *Xenopus laevis* oocytes.** *J. Lipid Res.* **2007.** 48: 1924–1935.

Supplementary key words mitochondria • reactive oxygen species • cell death • reduced glutathione

Sphingolipids are ubiquitous components of cellular membranes that play an essential role in the structural and functional properties of membranes. However, recent studies have documented the role of sphingolipids, in particular ceramide, in cell biology and in the regulation of multiple processes, including proliferation, cell growth/arrest, differentiation, and cell death (1). Regarding cell death, ceramide has been shown to block mitochondrial electron transfer, to stimulate the generation of reactive oxygen species (ROS), to depolarize mitochondria, and to induce the release of cytochrome c to activate caspases (2–4). The production of ceramide can occur by de novo synthesis through the sequential activation of serine-palmitoyl transferase, ceramide synthetase, and dehydroceramide desaturase (1, 5–7). Ceramide can also arise from the hydrolysis of sphingomyelin by the activation of sphingomyelinases (SMases). Several inducing stimuli, such as death ligands of the tumor necrosis factor (TNF) family, chemotherapeutic agents, or bacterial/viral infection, among others, activate two major known types of SMases (7). The neutral sphingomyelinase (NSMase), with three mammalian isoforms cloned to date, exhibits an optimum pH of $\sim$7.5 and is membrane-bound and Mg^{2+}-dependent (8–10). On the other hand, acidic sphingomyelinase (ASMase), with an optimum pH of $\sim$4.8, is further subclassified into several isoforms, an endosomal/

lysosomal ASMase, a secretory Zn^{2+}-dependent ASMase, and a receptor-activated ASMase thought to facilitate the onset of signaling platforms in specific microdomains of the plasma membrane (11–13). These enzymes contribute to the ability of the inducing stimuli to generate ceramide with different kinetics and, most likely, at different intracellular locations (14, 15).

The contribution of individual SMases to the biological effects of ceramide, particularly as a second messenger in cell death pathways, is determined by factors such as the kind of stimuli used and the cell type examined. For instance, NSMase has been shown to play a role in chemotherapy-mediated cell death (16), in the control of postnatal growth and differentiation (17), and in TNF-induced cell death in breast cancer cells (18). On the other hand, ASMase has been shown to play an essential role in the hepatocellular death signaling of TNF (19, 20), and ASMase deficiency has been shown to impair oocyte maturation and apoptosis caused by ionizing radiation (21). Moreover, ASMase has been shown to contribute to Fas-mediated cell death in hepatocytes but not in T-lymphocytes (22). Another factor, which may control the biological actions of SMase-induced ceramide, is the physicochemical properties of this lipid, which limit the intracellular diffusion of ceramide as a result of its almost negligible solubility, suggesting that the topology/sidedness of ceramide generation determines its actions. One of the best examples to illustrate this point is the reported effect of NSMase on the fate of the human T-cell lymphoma cell line Molt-4 (23). Incubation of Molt-4 cells with exogenous *Bacillus cereus* sphingomyelinase (bSMase) failed to induce apoptosis despite the increase of ceramide levels, whereas its stable transfection and induction caused poly (ADP-ribose) polymerase cleavage and cell death (23). In addition, the specific targeting of bSMase to mitochondria but not to other cell compartments in MCF breast cancer cells has been reported to lead to apoptosis (24). Whether these differential outcomes observed with bSMase in cancer cell lines reflect a general phenomenon that can be recapitulated in other cell types has not been investigated.

Xenopus laevis oocytes offer the advantage of being easily microinjected with exogenous metabolites (25–27), and the biochemical events of mammalian apoptosis have been recapitulated in cell-free extracts and in intact oocytes from *X. laevis* (28–31). Previous findings have reported that progesterone, a potent inducer of oocyte maturation, activated the sphingomyelin cycle (32) and that the incubation of *X. laevis* oocytes with exogenous NSMase from *Staphylococcus aureus* triggered their maturation (32, 33). Because, to the best of our knowledge, the role of bacterial NSMase microinjection in *X. laevis* oocytes has not been reported, here we examined the effects of incubation versus microinjection of bSMase on the maturation or apoptosis of *X. laevis* oocytes to further extend the concept of topologically restricted pools of ceramide associated with specific physiological responses (23, 24). Our findings show that bSMase induces both the meiotic cell cycle progression and apoptosis by an oxidant-dependent mech-anism in *X. laevis* oocytes, depending on the intracellular site where ceramide is generated.

EXPERIMENTAL PROCEDURES

Materials

Collagenase type IA, progesterone, bSMase, acidic sphingo-myelinase from human placenta (hSMase), ceramide C_8, pregnant mare serum gonadotropin, cytochrome c, reduced glutathione (GSH), and GSH-ethyl ester were purchased from Sigma (Madrid, Spain). Ceramide C_{16} and ceramide C_{18} were from Matreya. Caspase-3 substrate, Ac-Asp-Glu-Val-Asp-7-amino-4-trifluoromethyl coumarin (Ac-DEVD-AMC), caspase-3 inhibitor, Ac-Asp-Glu-Val-Asp-CHO (Ac-DEVD-CHO), and anti-Smac/Diablo antibody were from Calbiochem. [^{14}C]inulin (1.5 Ci/ml) was from American Radiolabeled Chemicals, Inc. *X. laevis* females were purchased from Centre National de la Recherche Scien-tifique, Montpellier, France and kept under standard conditions as described (25–27). Experimental protocols met the guide-lines of the Animal Care Committee of the Hospital Clinic Universidad de Barcelona.

Oocyte isolation and maturation

Female *Xenopus* frogs were primed by injection of pregnant mare serum gonadotropin (100 units) into the dorsal lymph sac 3 days before isolation. Ovaries were surgically removed from tricane-anesthetized frogs and dissected into small tissue sec-tions that were incubated in modified Barth's (MB) medium minus calcium (88 mM NaCl, 1 mM KCl, 2.4 mM NaHCO$_3$, 0.82 mM MgSO$_4$, and 15 mM HEPES, pH 7.6). Follicle cells were removed by incubating oocytes for 1–2 h with collagenase type IA (1 mg/ml) in modified Barth's medium containing calcium [0.33 mM Ca(NO$_3$)$_2$ and 0.41 mM CaCl$_2$]. Stage VI defolliculated oocytes (1–1.2 mm in diameter) were selected as described pre-viously (24–27) and stored in modified Barth's medium plus cal-cium supplemented with penicillin (100 U/ml), streptomycin (10 U/ml), gentamicin (50 ng/ml), and 0.250 μg/ml fungizone and maintained at 18°C with daily changes of medium. Germinal vesicle breakdown (GVBD) was monitored as a measure of matura-tion by the formation of a small white spot in the animal hemi-sphere of the oocyte. In addition, oocytes were fixed in 10% trichloroacetic acid and dissected to verify the absence of the germinal vesicle. In some cases, the levels of histone H1 kinase were determined as described before (32).

Treatment and microinjection with SMases and ceramides and oocyte fractionation

Oocytes with an intact vitelline envelope were incubated or microinjected with bSMase and hSMase (0.1–2 U/ml) using a computerized pressure-controlled microinjector (Atto Instru-ments, Potomac, MD). Control oocytes were microinjected with 30–50 nl/oocyte water or heat-inactivated SMase as a control. Final intracellular concentrations of the microinjected SMases were calculated considering the cytosolic volume of oocytes as ~1 μl. Groups of 100 oocytes were washed three times with mannitol isolation buffer containing 210 mM mannitol, 60 mM sucrose, 10 mM KCl, 10 mM succinic acid, 5 mM EGTA, and 10 mM HEPES-KOH (pH 7.5), supplemented with the protease inhibitors aprotinin and leupeptin at 10 μg/ml each, and finally homogenized in 1 volume of mannitol isolation buffer after 10 strokes using a 2 ml micro Dounce homogenizer. Extracts were centrifuged at 800 g followed by 9,000 g for 10 min to obtain a cytosolic fraction and a crude mitochondrial pellet. Purified

mitochondria were obtained through sucrose gradient centrifugation as described previously (26, 27). Mitochondrial purity was confirmed by the specific activity of succinate dehydrogenase in the final mitochondrial fraction with respect to homogenate. Mitochondrial ceramide levels were determined in isolated mitochondria from microinjected oocytes as described previously (2). In some cases, oocytes were microinjected with C_{16}-ceramide and C_{18}-ceramide (40–100 pmol/oocyte) or vehicle dodecane-ethanol (2:98, v/v) to examine their effects on cell death.

Western blot analysis of cytochrome c and Smac/Diablo

Proteins (40 μg) from cytosolic supernatants and mitochondrial pellets were separated by SDS-PAGE (15% gel) and transferred to nitrocellulose filters. Blots were probed with anti-cytochrome c (mouse monoclonal antibody; clone 7H8.2C12; dilution, 1:2,000 from Pharmigen) and anti-Smac/Diablo (rabbit polyclonal antibody; dilution, 1:1,000 from Calbiochem) antibodies. After 1 h of incubation with the primary antibody, bound antibodies were visualized with photographic film using horseradish peroxidase-coupled secondary antibodies and the ECL developing kit (Amersham Biosciences). Parallel aliquots were analyzed by immunoblotting for the release of cytochrome oxidase using monoclonal anti-cytochrome oxidase subunit II antibody to confirm the specificity of mitochondrial protein release.

Caspase activation

Cytosolic extracts were used to measure caspase-3 activity from the release of 7-amino-4-trifluoromethyl coumarin from Ac-DEVD-AMC, and fluorescence was continuously recorded with excitation at 380 nm and emission at 460 nm as described previously (34).

Determination of cellular oxidant production and GSH content

Reactive species formation was measured using chloromethyl-2′-7′-dichlorofluorescein diacetate (Molecular Probes, Eugene, OR), which becomes highly fluorescent upon oxidation by peroxides (35, 36), as well as peroxynitrite (37). Diclorofluorescein formation was continuously recorded in a fluorimeter with excitation at 503 nm and emission at 529 nm. Results were expressed as relative fluorescence units per microgram of protein. At various time points ranging from 0 to 24 h, GSH levels from oocyte homogenates, mitochondria, or cytosol were determined by high-performance liquid chromatography as described (38).

Cell viability by the inulin-release assay

Viability was followed by morphological assessment with a microscope, examining the appearance of the animal and vegetable hemispheres for lack of spots. In addition, we developed a quantitative method to estimate the leakiness of the plasma membrane to inulin. Water-treated controls or bSMase/hSMase-treated oocytes were microinjected with [^{14}C]inulin (American Radiolabeled Chemicals, Inc.; 1.5 Ci/ml), and cell death was determined by the release of labeled inulin to the medium and expressed as a percentage of the release caused by Triton X-100 (100% release).

Measurement of ceramide and SMase activity determination

Groups of 300 oocytes treated with SMases or vehicle were collected in liquid nitrogen at various times. Cellular levels of ceramide were determined by the diacylglycerol kinase assay after TLC using CHCl$_3$/CH$_3$COOH (9:1, v/v) or HPLC after alkaline hydrolysis and derivatization of the sphingoid base with

O-phthaldehyde after deacylation of ceramide, as described previously (34). Briefly, lipids were extracted with CH$_3$OH/CHCl$_3$ (2:1, v/v), and the organic phase was resuspended in 1 N KOH in methanol and incubated for 1 h at 100°C, yielding free sphingoid base, followed by derivatization with O-phthaldehyde. Samples were analyzed by HPLC in a reverse-phase C18 column (Waters) using a fluorimetric detector.

Mg^{2+}-dependent NSMase as well as ASMase activities were determined by monitoring [N-methyl-^{14}C]sphingomyelin (56.6 mCi/mmol; Amersham Biosciences) hydrolysis as described before (34). To measure NSMase, oocyte pellets were dissolved in a buffer containing 20 mM HEPES, pH 7.4, 10 mM MgCl$_2$, 2 mM EDTA, 5 mM DTT, 0.1 mM Na$_3$VO$_4$, 0.1 mM Na$_2$MoO$_4$, 30 mM p-nitrophenylphosphate, 10 mM β-glycerophosphate, 750 μM ATP, 1 mM PMSF, 10 mM leupeptin, 10 μM pepstatin, and 0.2% Triton X-100. After incubation for 5 min at 4°C, oocytes were homogenized by repeatedly squeezing the cells through an 18 gauge needle. Nuclei and cell debris were removed by low-speed centrifugation (800 g). Supernatants (30–50 μg of protein) were incubated for 2 h at 37°C in a buffer containing 20 mM HEPES, 1 mM MgCl$_2$ (pH 7.4), and 2.25 μl of [N-methyl-^{14}C]sphingomyelin. To measure ASMase, oocyte pellets were resuspended in 200 μl of 0.2% Triton X-100 and incubated for 15 min at 4°C, followed by centrifugation in a microfuge at 14,000 rpm for 10 min at 4°C. Supernatants (30–50 μg of protein) were incubated for 2 h at 37°C in a buffer (50 μl final volume) containing 250 mM sodium acetate, 1 mM EDTA (pH 5.0), and 2.25 μl of [N-methyl-^{14}C]sphingomyelin. In both assays, before measuring NSMase and ASMase activities, labeled sphingomyelin in detergent-mixed micelles was prepared by dissolving sphingomyelin, dried under nitrogen, with 0.2% Triton X-100 in neutral (20 mM HEPES and 1 mM MgCl$_2$, pH 7.4) or acidic (250 mM sodium acetate and 1 mM EDTA, pH 5.0) buffer, respectively. The preparations were sonicated in a warm bath until a clear solution was obtained and added freshly to the samples. Phosphorylcholine was extracted with 800 μl of chloroform-methanol (2:1, v/v) and 250 μl of water, identified by thin-layer chromatography, and routinely determined by scintillation counting.

Protein assay

Protein was measured using the Bio-Rad Protein Assay Kit (Bio-Rad) according to the manufacturer's protocol.

Statistical analyses

Results are expressed as means ± SD. Data were analyzed using a one-way ANOVA with Bonferroni corrections for multiple comparisons or a Student's t-test. $P < 0.05$ was considered statistically significant.

RESULTS

Ceramides are found in nature with N-fatty acyl chains containing from 2 to 28 carbon atoms that are linked to sphinganine via amide and alkyl linkages, the C_{16} to C_{24} species being more abundant than those containing C_2 to C_6 fatty acids. In addition to their relative abundance, a fundamental difference between long versus short ceramides is their solubility, so that ceramides with fatty acids C_{12} and longer have a very limited intracellular diffusion. This inherent physicochemical property of long fatty acid-containing ceramides suggests that the topology and membrane-sidedness of generation determine their bio-

logical effects (39). The generation of ceramides within membranes, however, induces major effects on the behavior of phospholipids, including lateral phase separation and domain formation, induction of transbilayer (flip-flop) lipid movements, and membrane permeabilization, which account for the biological effects of ceramides (7, 40–43).

Dual role of bSMase in maturation and cell death in *X. laevis* oocytes

To test the hypothesis that the sidedness of ceramide generation determines its biological effects, we compared the fate of *X. laevis* oocytes after incubation or microinjection with bSMase. Similar to previous findings with defolliculated oocytes incubated with *S. aureus* SMase (32, 33), the incubation of oocytes with bSMase (0.25 U/ml) caused the appearance of a white spot in the animal pole indicative of GVBD that reflects meiotic cell cycle progression (**Fig. 1A**). These findings were indistinguishable from those elicited by progesterone, the physiological inducer of maturation, suggesting that extracellular bSMase induced meiosis in *X. laevis* oocytes. Time-dependent studies indicated that GVBD started by 4 h of incubation with either bSMase or progesterone, with 90–95% of oocytes exhibiting GVBD by 8 h after treatment (Fig. 1B). However, because GVBD can also reflect a degenerative process rather than meiosis in response to specific treatments (44), we examined the activation of histone H1 kinase. As seen, the time-dependent pattern of histone H1 kinase after GVBD was similar in oocytes incubated with exogenous bSMase or progesterone (Fig. 1C), confirming meiotic maturation, in agreement with previous findings (32).

To check that the extracellular incubation of oocytes with bSMase increased ceramide levels, oocytes were homogenized and processed for ceramide determination by the diacylglycerol kinase assay and HPLC, with both approaches showing similar kinetics (Fig. 1D, E). Higher concentrations of bSMase (0.40–1.0 U/ml) accelerated ceramide generation (950–1,200 pmol/oocyte within 4–6 h) and the onset of GVBD (data not shown). Consistent with the meiotic maturation caused by incubation with bSMase, we observed that extracellular bSMase did not exert any cytotoxic effect in oocytes, as reflected by their morphologic appearance (Fig. 1A). Furthermore, to confirm the intactness of the plasma membrane after incubation with bSMase, we determined the amount of inulin released in the medium as a percentage of the release caused by the treatment of oocytes with Triton X-100. As seen, the percentage of inulin released from oocytes incubated with bSMase did not differ from that in vehicle-treated oocytes, whereas the microinjection of cytochrome c, which has been shown to induce apoptosis in oocytes (30), caused the release of inulin over time that approached 90–100% between 12 and 24 h (Fig. 1F). Furthermore, extracellular incubation of oocytes with bSMase did not result in the release of cytochrome c from mitochondria (**Fig. 2A**) or in the generation of ROS or GSH depletion (data not shown), confirming a lack of cytotoxic effects. Thus, extracellular bSMase-induced ceramide signals oocyte maturation and GVBD, confirming previous results with NSMase from *S. aureus* (32, 33, 45).

Because the effects of NSMase microinjection in *Xenopus* oocytes have not been reported, we examined the effect of microinjection of bSMase into oocytes on GVBD/cell death. To ensure the injection of an equivalent amount of bSMase as that used for the incubation experiments, and assuming that the volume of stage VI oocytes (1–1.2 mm diameter) is 0.8–1.0 µl, we injected 50 nl of 5 U/ml bSMase into oocytes (0.00025 unit of bSMase per oocyte, equivalent to 0.250 U/ml oocyte volume). Microinjection of bSMase increased the intracellular levels of ceramide time-dependently (Fig. 2B, C), which resulted in the appearance of transparent blisters, mottled spots on the cell surface, and the blurring of the sharp border between the animal and vegetable poles, indicative of cytotoxicity (Fig. 2D). bSMase microinjection generated higher ceramide levels compared with the incubation of oocytes with an equivalent amount of extracellular bSMase (Figs. 1E, 2C). However, increasing levels of extracellular bSMase (0.4–1.0 U/ml), which generated similar ceramide levels as those seen after bSMase microinjection (Fig. 2B, C), were not cytotoxic to oocytes, based on the lack of inulin release but accelerated GVBD (data not shown). The inulin assay revealed the gradual loss of the membrane intactness over time induced by microinjection of bSMase (Fig. 2E).

To examine whether these effects were dose-dependent, oocytes were injected with 50 nl of 0.5 or 2.5 U/ml bSMase, to yield an estimated amount of 0.025 and 0.125 unit of bSMase per milliliter of oocyte volume, respectively, resulting in a proportional increase of the intracellular ceramide levels over time (Fig. 2C) that translated to a dose-dependent release of inulin, indicative of cell death (Fig. 2E). As an additional control, we microinjected oocytes with heat-inactivated bSMase to check for nonspecific effects. Microinjection of inactivated bSMase (0.250 U/ml) did not increase ceramide levels in mitochondria (Fig. 2F) and was not cytotoxic to oocytes, as seen by the lack of release of cytochrome c from mitochondria (Fig. 2A) and by the inulin assay (Fig. 2E). Moreover, the generation of ceramide after bSMase microinjection was associated with purified mitochondria isolated from microinjected oocytes versus water-injected oocytes, as opposed to when oocytes were incubated with exogenous bSMase (Fig. 2F).

We also examined whether these effects were specific for bSMase and tested the role of hSMase, an ASMase from human placenta previously reported to induce apoptosis in primary hepatocytes (34). hSMase microinjection resulted in oocyte death, determined by their macroscopic appearance and by the inulin assay, although these effects occurred with slower kinetics compared with the effects observed with bSMase (**Fig. 3A, B**). Interestingly, however, incubation of oocytes with hSMase did not cause GVBD or cell death (data not shown), consistent with the inability of extracellular hSMase to generate ceramide. Furthermore, the microinjection of C_{16} and C_{18} ceramide (40–100 pmol/oocyte) but not the vehicle alone (dodecane-ethanol, 2:98) induced oocyte death based on their
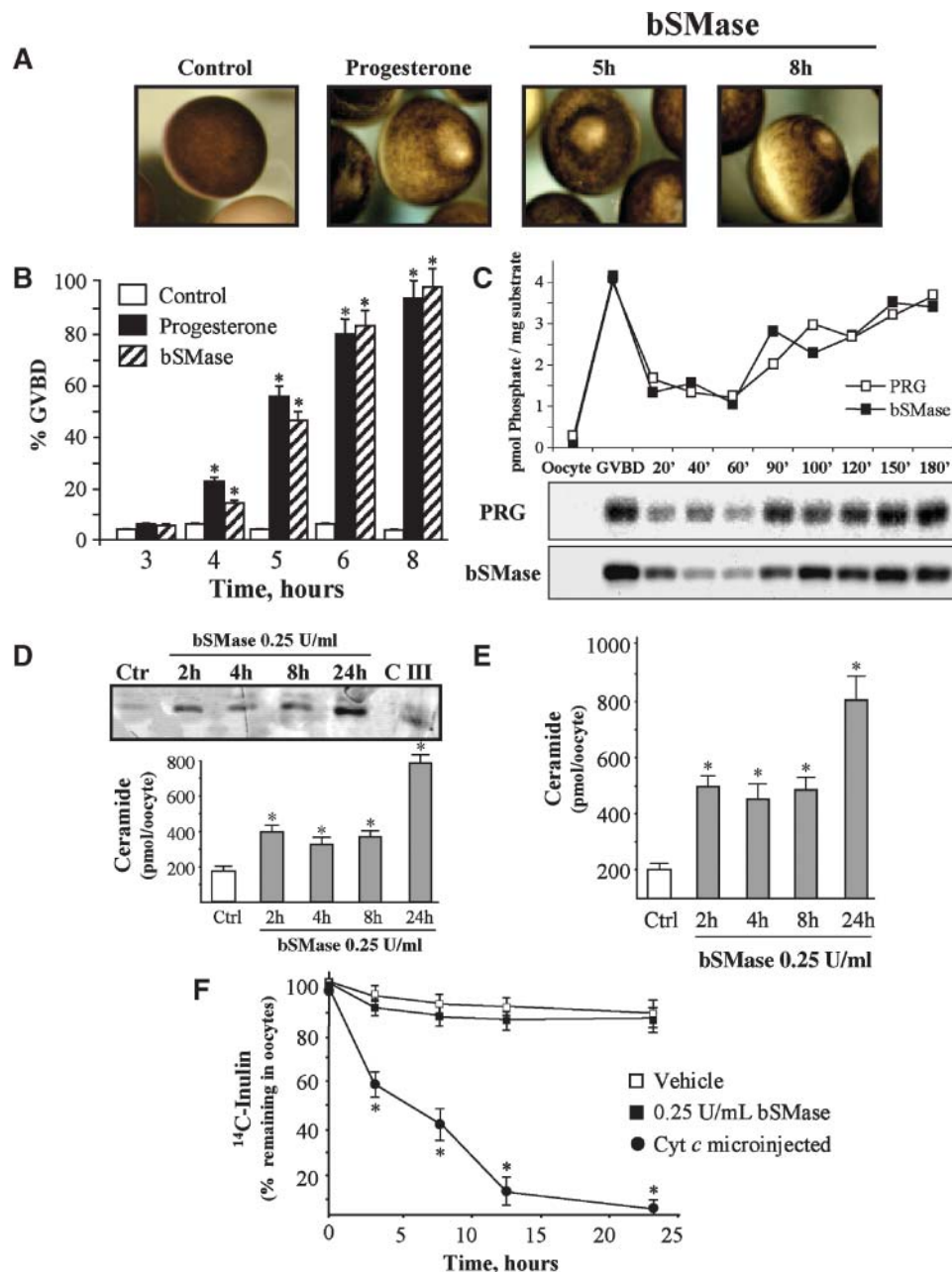
Fig. 1. Effect of *Bacillus cereus* sphingomyelinase (bSMase) incubation on oocyte maturation. A: Morphological appearance of oocytes after exposure to progesterone (10 µg/ml) and bSMase (0.25 U/ml), as indicated in Experimental Procedures, showing the germinal vesicle breakdown (GVBD) as the white spot in the animal pole. B: Batches of 20–30 oocytes were incubated with progesterone and bSMase to examine the kinetics of GVBD as shown in A. Results are means ± SD of three to four independent experiments. * $P < 0.05$ versus control oocytes. C: Time-dependent histone H1 kinase in oocytes incubated with progesterone (PRG) or bSMase for the indicated times. Extracts were collected and processed for H1 kinase assay as described previously (32). The time-dependent changes of H1 kinase activity of the progesterone- and bSMase-treated oocytes were significant ($P < 0.05$) with respect to basal oocytes and those exhibiting GVBD, without significant differences between the progesterone and bSMase groups. D: Oocytes were treated with bSMase (0.25 U/ml), and samples were collected at the time intervals indicated and assayed for ceramide using diacylglycerol kinase using CIII as a ceramide standard. A representative TLC plate and its quantification, out of three independent experiments, are shown. Results are means ± SD. * $P < 0.05$ versus control oocytes. E: Oocyte extracts after bSMase treatment were processed for the determination of ceramide by HPLC. Results are means ± SD of three different experiments. * $P < 0.05$ versus control oocytes. F: Oocytes were microinjected with [^{14}C]inulin to check the intactness of the plasma membrane after treatment with bSMase. Cytochrome c microinjection (10 µM) was used as a positive control of cell death. Results are means ± SD. * $P < 0.05$ versus control oocytes.
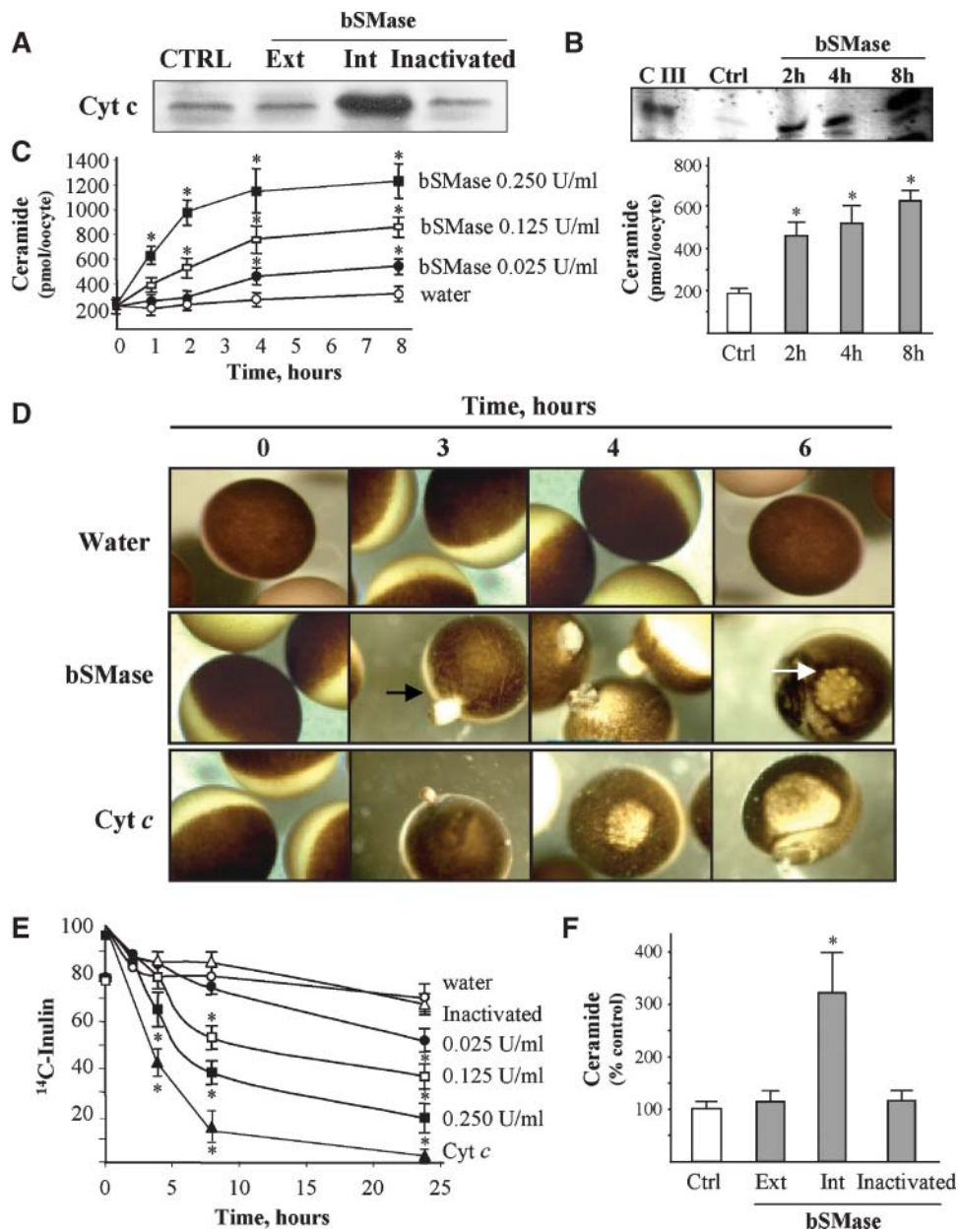
Fig. 2. bSMase microinjection kills oocytes. A: Oocytes were incubated with extracellular bSMase (Ext) as in Fig. 1, or microinjected with active bSMase (Int) or heat-inactivated enzyme (Inactivated), and cytochrome c release in cytosolic extracts was assessed by Western blot. A representative blot of three independent experiments showing similar results is shown. B: Oocytes were microinjected with bSMase (50 nl of a 5 U/ml stock), and samples were collected at the time intervals indicated and assayed for ceramide using diacylglycerol kinase using CIII as a ceramide standard. A representative TLC plate and its quantification, out of three independent experiments, are shown. Results are means ± SD. * $P < 0.05$ versus water-injected oocytes. C: Oocyte extracts after microinjection with different doses of bSMase were processed for the determination of ceramide by HPLC. Results are means ± SD of three different experiments. * $P < 0.05$ versus water-injected oocytes. D: Oocytes were microinjected with bSMase or cytochrome c and examined morphologically at various times. As seen, instead of the characteristic white spot in the animal pole reflecting GVBD, cells exhibited signs of cytotoxicity, including ruptured blisters and mottled spots on the cell surface (arrows). E: Oocytes were microinjected with bSMase or water along with [^{14}C]inulin to examine its release in the medium over time. Results are means ± SD of three to four independent experiments. * $P < 0.05$ versus water-injected oocytes. F: Mitochondrial ceramide levels from oocytes treated with extracellular bSMase or microinjected with active or heat-inactivated bSMase for 2 h, as described for A. Ceramide levels were determined by HPLC. Results are means ± SD of three different experiments. * $P < 0.05$ versus water-injected oocytes.
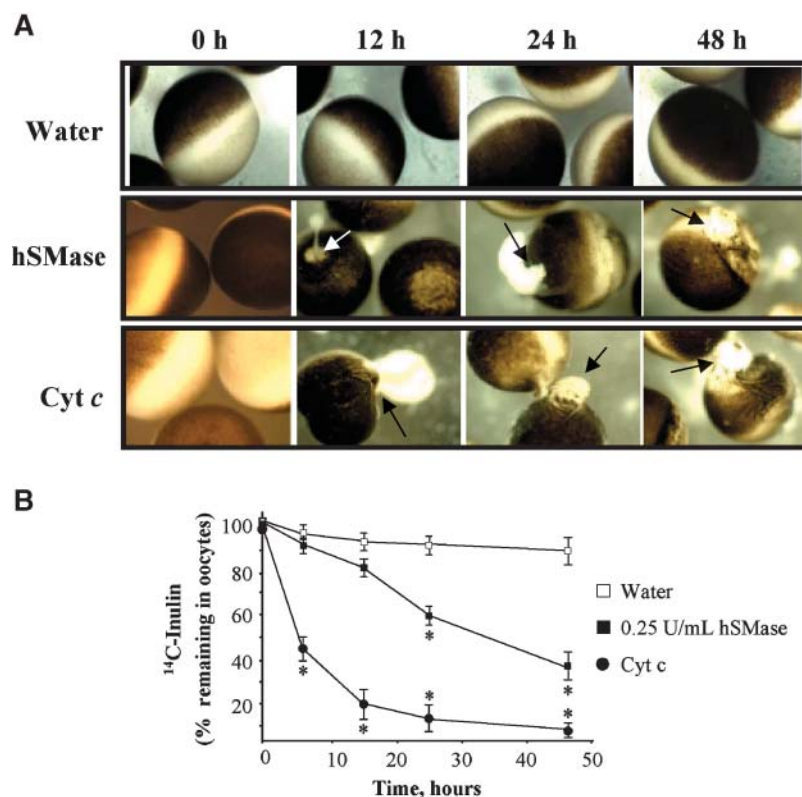
Fig. 3. Effects of human placenta sphingomyelinase (hSMase) microinjection in oocytes. A: Oocytes were microinjected with 50 nl of a 5 U/ml stock solution of hSMase (equivalent to 0.25 unit of hSMase per milliliter of oocyte volume) as well as cytochrome *c*, as a positive control, and examined macroscopically for cytotoxicity, as indicated by the arrows. Representative images out of four independent experiments are shown. B: Oocytes were microinjected with hSMase (0.25 U/ml) or water (50 nl) along with [^{14}C]inulin to examine its release in the medium over time. Results are means ± SD of three to four independent experiments. * $P < 0.05$ versus water-injected oocytes.

macroscopic appearance and inulin release (67 ± 7% vs. 12 ± 6% inulin release for C_{16} ceramide and solvent-injected oocytes, respectively). Thus, these findings show the differential outcome of bSMase in the maturation or death of *Xenopus* oocytes, depending whether bSMase was added extracellularly or microinjected, and suggest that the ceramide produced by either approach likely occurred in different cellular locations.

bSMase microinjection induces oocyte apoptosis by an oxidant-dependent mechanism

Having observed that the microinjection but not the incubation of bSMase was cytotoxic to oocytes, we next addressed the mechanism and the biochemical features of oocyte death after bSMase microinjection. We focus on the generation of ROS and GSH homeostasis, as these factors are known to regulate cell death (46) and because ceramide has been shown to target mitochondria to stimulate ROS generation (2–4). bSMase microinjection resulted in a dose-dependent generation of ROS that increased gradually from 4 to 8 h after injection, declining by 10 h (**Fig. 4A**). This response was accompanied by the depletion of total GSH equivalents in both the cytosol and mitochondrial fractions of microinjected oocytes (Fig. 4B, C). To examine whether the reduction in the intracellular

GSH levels was attributable to its efflux out of oocytes, we measured GSH equivalents in the medium. As seen, the appearance of GSH in the extracellular medium did not account for the depletion of total GSH levels in oocyte extracts (Fig. 4D), suggesting the net consumption of GSH equivalents upon bSMase injection. These findings underscore the ability of bSMase to induce oxidative stress and the generation of ROS, which in turn consume GSH equivalents.

Because several biochemical events of mammalian apoptosis occur in *Xenopus* oocytes, we next examined whether bSMase activated the mitochondrial apoptosome. Oocytes were fractionated, and the cytosol fraction was examined for the release of apoptogenic proteins such as cytochrome c and Smac/Diablo. As seen, bSMase injection resulted in the release of both proteins from mitochondria to the cytosol in a time-dependent manner (**Fig. 5A**). This effect was specific for cytochrome c and Smac/Diablo, as other mitochondrial proteins were not released into the cytosol (Fig. 5A). Because this event is critical in the cytosolic activation of downstream caspases, we monitored the activity of caspase-3 in cytosolic extracts from oocytes microinjected with bSMase. bSMase injection dose-dependently activated caspase-3, as reflected by the increase over time of the AMC fluorescence (Fig. 5B) as
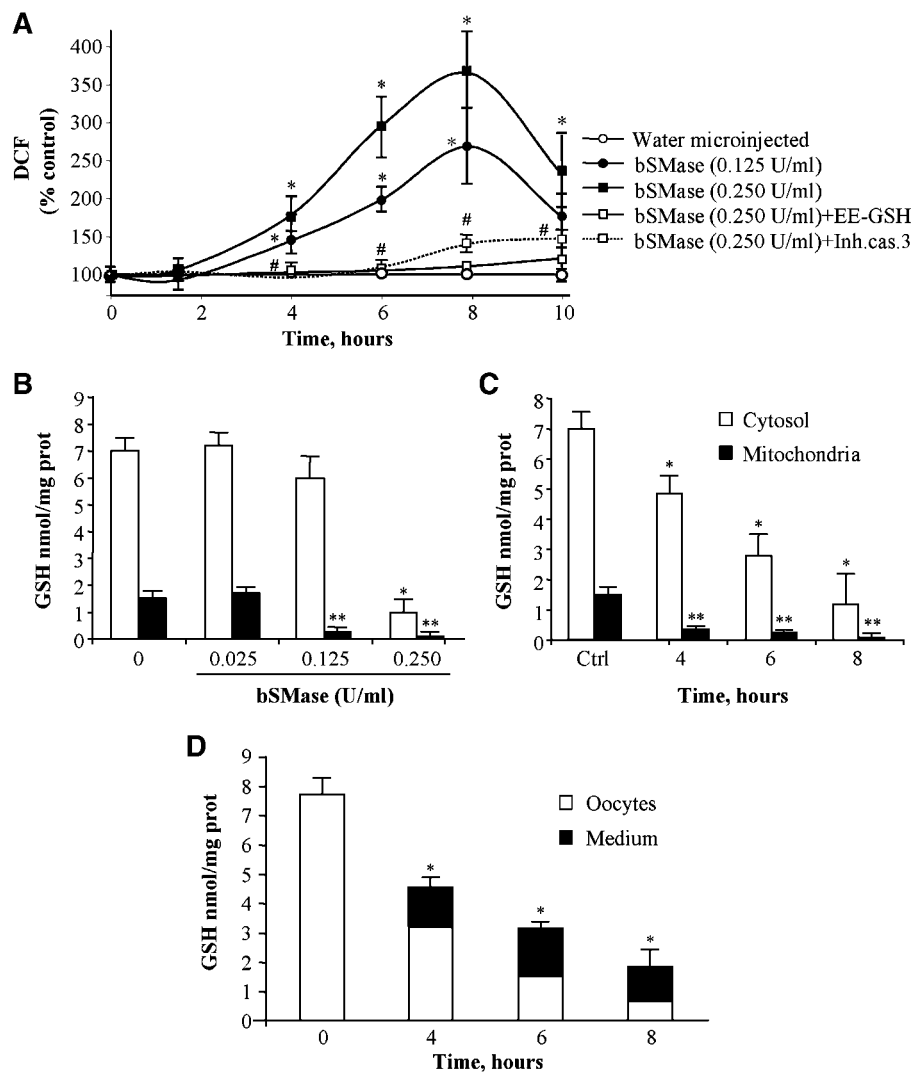
Fig. 4.   Increased reactive oxygen species (ROS) generation and reduced glutathione (GSH) depletion by microinjected bSMase. A: ROS were determined from diclorofluorescein fluorescence at different times after oocytes were microinjected with different doses of bSMase. The oocytes were mechanically disrupted and prepared as described in Experimental Procedures to determine diclorofluoresceinfluorescence. Results are means ± SD of five independent experiments. * $P < 0.05$ versus control; [#] $P < 0.05$ versus bSMase alone. B: Dose response of cytosolic and mitochondrial GSH levels in oocytes injected with bSMase after 8 h. Results are means ± SD of four independent experiments. * $P < 0.05$ versus cytosol GSH from control oocytes; ** $P < 0.05$ versus mitochondrial GSH from control oocytes. C: Time-dependent depletion of GSH levels in oocytes injected with bSMase at 0.25 U/ml. Oocytes were fractionated into cytosol and mito-chondria to determine GSH levels. Results are means ± SD of three different experiments. * $P < 0.05$ versus control cytosol GSH; ** $P < 0.05$ versus control mitochondrial GSH. D: GSH equivalents were determined in oocytes and medium at different time intervals after bSMase (0.25 U/ml) microinjection. Results are means ± SD of at least three different experiments. * $P < 0.05$ versus control.

well as by immunoblotting with the appearance of active fragments (data not shown). Moreover, microinjection of heat-inactivated bSMase failed to activate caspase-3 (Fig. 5B). These mitochondria-dependent events coincided with the onset of oocyte death induced by bSMase injection (Fig. 2E).

Furthermore, because GSH regulates apoptotic pathways, we examined whether GSH-ethyl ester preincubation abolishes the apoptotic effect of bSMase microinjection. GSH-ethyl ester enhanced the total GSH levels compared with basal oocytes (**Fig. 6A**), and more importantly, it pre-

vented the generation of ROS (Fig. 4A) and the release of cytochrome c and Smac/Diablo from mitochondria as well as caspase-3 activation (Fig. 6B, C). Consistent with these observations, the preincubation with GSH-ethyl ester protected oocytes against bSMase-induced cell death (Fig. 6D), similar to the rescue afforded by the caspase-3 inhibitor Ac-DEVD-CHO (Fig. 6D), which also attenuated the generation of ROS by bSMase microinjection (Fig. 4A). The mechanism of protection by GSH in this paradigm is of interest. Previous findings reported that GSH inhibits the activity of NSMase (47). However, GSH-
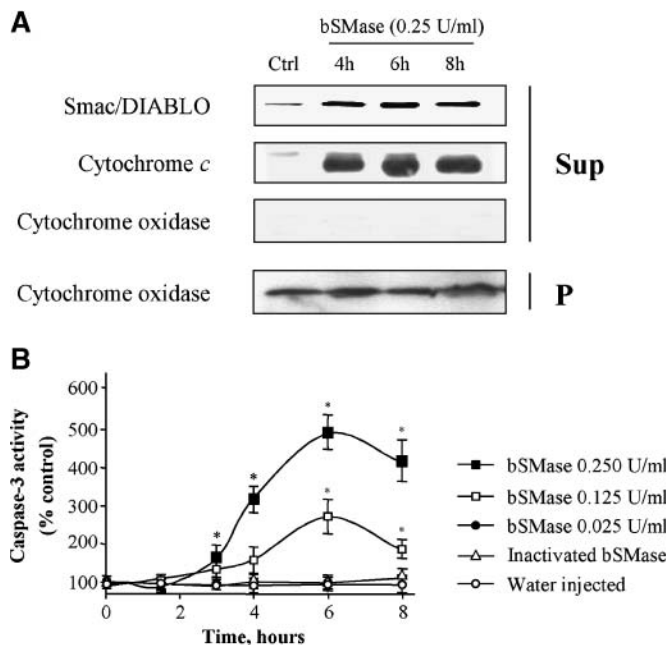
Fig. 5. Neutral SMase microinjection stimulates the release of mitochondrial proapoptotic factors and caspase-3 activation. A: Oocytes were microinjected with bSMase (0.25 U/ml) and after 4, 6, and 8 h, oocytes were fractionated into mitochondria [pellet (P)] and cytosol [supernatant (Sup)]. Both the pellet and supernatant were analyzed by Western blot using anti-cytochrome c antibody and anti-Smac/Diablo antibody followed by appropriate secondary antibodies. The specificity of mitochondrial release was confirmed in parallel aliquots from pellets and supernatants using anti-cytochrome c oxidase antibody. B: Oocytes were microinjected with several doses of bSMase as shown, and caspase-3 activity was measured with oocyte total extracts prepared as described in Experimental Procedures. Results are means ± SD of three different experiments. * $P < 0.05$ versus control.

ethyl ester preincubation did not inhibit bSMase, because it did not prevent the generation of ceramide induced by bSMase (Fig. 6E). Rather, the consequences of ceramide generation by bSMase, such as ROS overgeneration and mitochondrial release of proapoptotic proteins, were blocked by increasing GSH levels with GSH-ethyl ester, consistent with prior observations in different cell types, in which the cellular loss of GSH preceded the onset of apoptosis induced by death ligands (48, 49).

The fact that caspase inhibition blocks bSMase-induced ROS generation deserves further comment, as it implies that ROS production occurs downstream of caspase activation. Recent findings have indicated that fibroblasts deficient in downstream caspases were resistant to mitochondrial and death receptor-mediated apoptosis, exhibiting a preservation of mitochondrial membrane potential and defects in early mitochondrial apoptotic events, including Bax translocation and cytochrome c release (50). Although mitochondrial targeting by bSMase-induced ceramide generation may contribute to ROS generation, cytochrome c release, and caspase activation, active caspases (e.g., caspase-3) may, in turn, engage in an amplification loop acting on mitochondria to further stimulate ROS generation, mitochondrial dysfunction, and caspase acti-

vation, consistent with the ability of caspase-3 inhibition to break these events.

DISCUSSION

We have exploited *Xenopus* oocytes as a cellular tool to test and expand the concept regarding the availability of distinct pools of ceramide functionally linked to divergent physiological responses. First described in Molt-4 leukemia cells (23), it was shown that extracellular bSMase did not cause cell death, as opposed to its stable transfection despite the fact that both approaches generated similar cell-associated ceramide levels. Although this study and subsequent observations in MCF cells (24) proposed that the intracellular generation of ceramide in specific compartments activates apoptosis pathways, they also implied that the generation of ceramide in the outer leaflet of the plasma membrane was inactive, at least with regard to cell death induction. Although that pioneer study did not examine any other biological functions of ceramide when generated by extracellular bSMase, the incubation of *Xenopus* oocytes with bacterial SMase from either *B. cereus* (this study) or *S. aureus* signals oocyte maturation characterized by GVBD, histone H1 kinase activation, and pp34^{cdc2} (32, 33, 45). To account for this function, observations in model and cell membranes reported the flip-flop movement of ceramide (42, 43), gaining access to the inner leaflet of the plasma membrane to interact with specific targets. In agreement with this concept, extracellular NSMase from *S. aureus* has been shown to increase cytoplasmic Ca^{2+} via the inositol-3-phosphate receptor Ca^{2+} release channel on the endoplasmic reticulum, leading to oocyte maturation (51). Moreover, another study reported that the inhibition of glycosphingolipid synthesis by 1-phenyl-2-decanoylamino-3-morpholino-1-propanol (PDMP), an inhibitor of the glucosylceramide synthase (GCS) (52), activated p34^{cdc2} in *Xenopus* oocytes and induced GVBD and maturation (45). Intriguingly, because the inhibition of GCS by PDMP can lead to increased intracellular ceramide levels by preventing the conversion of ceramide to glucosylceramide (52), this raises the concern of whether the maturation caused by PDMP was attributable to increased intracellular ceramide or to the down-regulation of complex glycosphingolipids that may have played a role in this process (45). The immediate targets, however, that mediate the specific effect of ceramide generated from extracellular bSMase in GVBD and subsequent oocyte maturation remain to be identified.

We show that the intracellular generation of ceramide by bSMase into oocytes induces cell death by an oxidant-dependent mechanism that promotes the release of mitochondrial apoptotic proteins. Consistent with the involvement of ROS generation, oocyte GSH levels became depleted; furthermore, boosting GSH by GSH-ethyl ester protected oocytes against bSMase. These observations raise some questions in view of the reported reciprocal regulation of GSH and NSMase. Although the protection afforded by GSH replenishment via GSH-ethyl
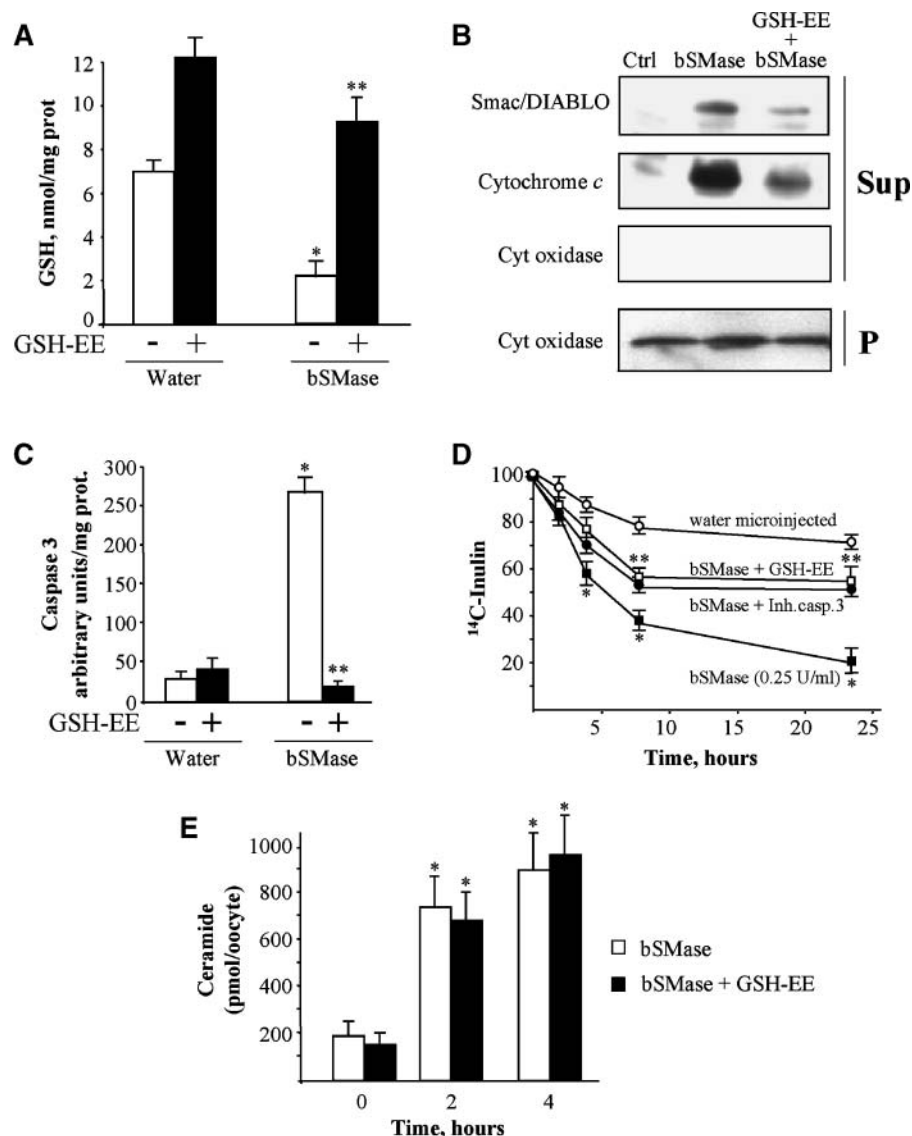
Fig. 6. GSH-ethyl ester (GSH-EE) prevents excessive ROS production, release of proapoptotic proteins, and oocyte death. A: Oocytes were preincubated with 10 mM GSH-ethyl ester at 1 h before microinjection with 0.25 U/ml bSMase, determining the levels of GSH in oocytes after treatment. Results are means ± SD of four different experiments. * $P < 0.05$ versus control; ** $P < 0.05$ versus bSMase-injected oocytes. B: Oocytes microinjected with bSMase with or without GSH-ethyl ester pretreatment were fractionated into cytosol and mitochondria to examine the release of Smac/Diablo and cytochrome c. C: Oocytes were processed as for Fig. 5B to examine the effect of GSH-ethyl ester pretreatment on bSMase-induced caspase-3 activation. Results are means ± SD of four different experiments. * $P < 0.05$ versus control; ** $P < 0.05$ versus bSMase-injected oocytes. D: Oocytes were injected with bSMase (0.25 U/ml) with or without preincubation with GSH-ethyl ester or with caspase-3 inhibitor and assayed for [14C]inulin release. Results are means ± SD of at least three different experiments. * $P < 0.05$ versus control, ** $P < 0.05$ versus bSMase alone. E: Oocyte extracts were prepared after bSMase microinjection with or without GSH-ethyl ester pretreatment (1 h) to determine the levels of ceramide by HPLC. Results are means ± SD of at least three different experiments. * $P < 0.05$ versus control oocytes. All time point were 8 h after bSMase microinjection.

ester could have been attributable to the inhibition of bSMase by GSH, as reported (47), GSH did not prevent the generation of ceramide after bSMase microinjection. Although the data reported by Liu and Hannun (47) was from partially purified NSMase from Molt-4 cells, interestingly, the enzyme purified from liver plasma membrane was not inhibited by GSH as opposed to ubiquinol (53), suggesting that the inhibition of NSMase by GSH does not

appear to be a general phenomenon but rather seems to be species-dependent or cell type-dependent. However, whether or not GSH inhibition of NSMase depends on an accessory protein is unknown.

Another question relates to the regulation of GSH by NSMase. We previously observed that the exposure of cultured rat hepatocytes to bSMase induced the expression of γ-GCS, the rate-limiting enzyme in GSH synthesis, result-

ing in enhanced hepatocellular GSH stores (34). This raises the possibility that the depletion of GSH stores in oocytes microinjected with bSMase may have occurred despite the putative induction of γ-GCS. However, although we did not examine the regulation of γ-GCS in oocytes after bSMase microinjection, it is conceivable that GSH depletion may occur in the face of γ-GCS induction. For instance, we previously observed that the exposure of primary hepatocytes to TNF resulted in increased ROS formation and GSH depletion, despite the fact that TNF stimulates the transcriptional activation of the γ-GCS heavy subunit (35). Our data regarding the ability of GSH-ethyl ester to inhibit ROS generation, GSH loss, and cell death but not ceramide imply that GSH might be downstream of ceramde generation after exogenous bSMase microinjection. However, in addition to this interpretation, it may be possible that bSMase microinjection could have induced the production of endogenous ceramide through other pathways. In this regard, we observed that microinjection of oocytes with myriocin or fumonisin did not block the cytotoxicity of microinjected bSMase reflected by the release of inulin, thus discarding the potential contribution of endogenous ceramide generation via de novo synthesis in the cytotoxic effects of bSMase. However, we cannot totally rule out the possibility that the activation of endogenous oocyte neutral SMase after bSMase microinjection may have contributed to the cytotoxicity of microinjected bSMase.

Overall, these data reflect the potential of bSMase-induced ceramide to induce oxidative stress and ROS production when generated intracellularly in oocytes by targeting mitochondria. Consistent with these findings, Birbes et al. (24) showed that the enforced targeting of bSMase into mitochondria but not other subcellular organelles results in the apoptosis of MCF cells. Interestingly, the effects of bSMase microinjection are recapitulated by microinjection of hSMase, an acidic SMase from human placenta previously reported to kill primary hepatocytes by an oxidant-dependent mechanism (34), with the generation of ROS from mitochondria that depletes net equivalents of GSH. In contrast to these observations in *Xenopus*, previous findings in mammalian cells (primary hepatocytes and human colon HT-29 cells) revealed a distinct outcome between the effects of extracellular bSMase and hSMase in apoptosis, with the putative apoptotic role of bSMase being modulated by nuclear factor-κB. Indeed, the inhibition of nuclear factor-κB before bSMase exposure unmasked the apoptotic potential of ceramide generated by extracellular bSMase (54). Interestingly, the kinetics of oocyte death caused by hSMase microinjection lagged behind that induced by bSMase. Because previous studies indicated the requirement of intracellular acidic vesicles to ensure hSMase activation and ceramide generation (20, 34), it is conceivable that the slower oocyte death caused by hSMase versus bSMase microinjection may reflect the trafficking of injected hSMase to appropriate acidic compartments. Although these data demonstrate the mitochondrial targeting by SMase-induced ceramide generation in oocytes, a remaining question is

whether ceramide is generated inside mitochondria through the hydrolysis of mitochondrial sphingomyelin, as suggested in the case of MCF cells treated with bSMase constructs (24), or is generated extramitochondrially and then traffics to this compartment to stimulate ROS and downstream events leading to cell death.

In summary, our data show the potential of *Xenopus* oocytes as a tool to investigate the biological effects of ceramide in relation to its topology of generation in addition to the use of model membranes, and they extend the concept that the site of ceramide generation is a major determinant of its biological actions. Although this notion was first observed in cancer cells, its confirmation in *Xenopus* oocytes ensures that topology-dependent ceramide function is a general phenomenon that may be exploited to design strategies to modulate the effects of ceramide on cell death.▪

REFERENCES

1. Hannun, Y. A., and C. Luberto. 2000. Ceramide in the eukaryotic stress response. *Trends Cell Biol.* **10:** 73–80.
2. Garcia-Ruiz, C., A. Colell, M. Mari, A. Morales, and J. C. Fernandez-Checa. 1997. Direct effect of ceramide on the mitochondrial electron transport chain leads to generation of reactive oxygen species. Role of mitochondrial glutathione. *J. Biol. Chem.* **272:** 11369–11377.
3. Gudz, T. I., K. Y. Tserng, and C. L. Hoppel. 1997. Direct inhibition of mitochondrial respiratory chain complex III by cell-permeable ceramide. *J. Biol. Chem.* **272:** 24154–24158.
4. Ghafourifar, P., S. D. Klein, O. Schucht, U. Schenk, M. Pruschy, S. Rocha, and C. Richter. 1999. Ceramide induces cytochrome c release from isolated mitochondria. Importance of mitochondrial redox state. *J. Biol. Chem.* **274:** 6080–6084.
5. Merrill, A. H., S. Lingrell, E. Wang, M. N. Nikolova-Karakashian, and D. Vance. 1995. Sphingolipid biosynthesis de novo by rat hepatocytes in culture. Ceramide and sphingomyelin are associated with, but not required for, very low-density lipoprotein secretion. *J. Biol. Chem.* **270:** 13834–13841.
6. Spiegel, S., and A. H. Merrill. 1996. Sphingolipid metabolism and growth regulation. *FASEB J.* **10:** 1388–1397.
7. Morales, A., H. Lee, F. M. Goñi, R. N. Kolesnick, and J. C. Fernandez-Checa. 2007. Sphingolipids and cell death. *Apoptosis.* **12:** 923–939.
8. Clarke, C. J., C. F. Snook, M. Tani, N. Matmati, N. Marchesini, and Y. A. Hannun. 2006. The extended family of neutral sphingomyelinases. *Biochemistry.* **45:** 11247–11256.
9. Marchesini, N., C. Luberto, and Y. A. Hannun. 2003. Biochemical properties of mammalian neutral sphingomyelinase 2 and its role in sphingolipid metabolism. *J. Biol. Chem.* **278:** 13775–13783.
10. Krut, O., K. Wiegmann, H. Kashkar, B. Yazdanpanah, and M. Kronke. 2006. Novel tumor necrosis factor-responsive mammalian neutral sphingomyelinase-3 is a C-tail-anchored protein. *J. Biol. Chem.* **281:** 13784–13793.
11. Schissel, S. L., X. Jiang, J. Tweedie-Hardman, T. Jeong, E. H. Camejo, J. H. Rapp, K. J. Williams, and I. Tabas. 1998. Secretory sphingomyelinase, a product of the acid sphingomyelinase gene, can hydrolyze atherogenic lipoproteins at neutral pH. Implications for atherosclerotic lesion development. *J. Biol. Chem.* **273:** 2738–2746.

12. Liu, P., and R. G. Anderson. 1995. Compartmentalized production of ceramide at the cell surface. *J. Biol. Chem.* **270:** 27179–27185.

13. Grassme, H., A. Cremesti, R. Kolesnick, and E. Gulbins. 2003. Ceramide-mediated clustering is required for CD95-DISC formation. *Oncogene.* **22:** 5457–5470.

14. Wiegman, K., S. Schutze, T. Machleidt, D. Witte, and M. Kronke. 1994. Functional dichotomy of neutral and acidic sphingomyelinase in tumor necrosis factor signalling. *Cell.* **78:** 1005–1015.

15. Kolesnick, R. N., and M. Kronke. 1998. Regulation of ceramide production and apoptosis. *Annu. Rev. Physiol.* **60:** 643–665.

16. Bezombe, C., I. Plo, V. Mansat-De Mas, A. Quillet-Mary, A. Negre-Salvayre, G. Laurent, and J. P. Jaffrezou. 2001. Lysosomal sphingomyelinase is not solicited for apoptotic signalling. *FASEB J.* **15:** 297–299.

17. Stoffel, W., B. Jenke, B. Blöck, M. Zumbansen, and J. Koebke. 2005. Neutral sphingomyelinase 2 (smpd3) in the control of postnatal growth and development. *Proc. Natl. Acad. Sci. USA.* **102:** 4554–4559.

18. Luberto, C., D. F. Hassler, P. Signorelli, Y. Okamoto, H. Sawai, E. Boros, D. J. Hazen-Martin, L. M. Obeid, Y. A. Hannun, and G. K. Smith. 2002. Inhibition of tumor necrosis factor-induced cell death in MCF-7 by a novel inhibitor of neutral sphingomyelinase. *J. Biol. Chem.* **277:** 41128–41139.

19. Garcia-Ruiz, C., A. Colell, M. Mari, A. Morales, M. Calvo, C. Enrich, and J. C. Fernandez-Checa. 2003. Defective TNF-alpha-mediated hepatocellular apoptosis and liver damage in acidic sphingomyelinase knockout mice. *J. Clin. Invest.* **111:** 197–208.

20. Mari, M., A. Colell, A. Morales, A. Paneda, I. Varela-Nieto, C. Garcia-Ruiz, and J. C. Fernandez-Checa. 2004. Acidic sphingomyelinase downregulates the liver-specific methionine adenosyltransferase 1A, contributing to tumor necrosis factor-induced lethal hepatitis. *J. Clin. Invest.* **113:** 895–904.

21. Morita, Y., G. I. Perez, F. Paris, S. R. Miranda, D. Ehleiter, A. Haimovitz-Friedman, Z. Fuks, Z. Xie, J. C. Reed, E. H. Schuchman, et al. 2000. Oocyte apoptosis is suppressed by disruption of the acid sphingomyelinase gene or by sphingosine-1-phosphate therapy. *Nat. Med.* **6:** 1109–1114.

22. Lin, T., L. Genestier, M. J. Pinkoski, A. Castro, S. Nicholas, R. Mogil, F. Paris, Z. Fuks, E. H. Schuchman, R. N. Kolesnick, et al. 2000. Role of acidic sphingomyelinase in Fas/CD95-mediated cell death. *J. Biol. Chem.* **275:** 8657–8663.

23. Zhang, P., B. Liu, G. M. Jenkins, Y. A. Hannun, and L. M. Obeid. 1997. Expression of neutral sphingomyelinase identifies a distinct pool of sphingomyelin involved in apoptosis. *J. Biol. Chem.* **272:** 9609–9612.

24. Birbes, H., S. El Bawab, Y. A. Hannun, and L. M. Obeid. 2001. Selective hydrolysis of a mitochondrial pool of sphingomyelin induces apoptosis. *FASEB J.* **14:** 2669–2677.

25. Fernandez-Checa, J. C., J. R. Yi, C. Garcia-Ruiz, Z. Knezic, S. M. Tahara, and N. Kaplowitz. 1993. Expression of rat liver reduced glutathione transport in *Xenopus laevis* oocytes. *J. Biol. Chem.* **268:** 2324–2328.

26. Garcia-Ruiz, C., A. Morales, A. Colell, J. Rodes, J. R. Yi, N. Kaplowitz, and J. C. Fernandez-Checa. 1995. Evidence that the rat hepatic mitochondrial carrier is distinct from the sinusoidal and canalicular transporters for reduced glutathione. Expression studies in *Xenopus laevis* oocytes. *J. Biol. Chem.* **270:** 15946–15949.

27. Coll, O., A. Colell, C. Garcia-Ruiz, N. Kaplowitz, and J. C. Fernandez-Checa. 2003. Sensitivity of the 2-oxoglutarate carrier to alcohol intake contributes to mitochondrial glutathione depletion. *Hepatology.* **38:** 692–702.

28. Newmeyer, D. D., D. M. Farschon, and J. C. Reed. 1994. Cell-free apoptosis in Xenopus egg extracts: inhibition by Bcl-2 and requirement for an organelle fraction enriched in mitochondria. *Cell.* **79:** 353–364.

29. Kluck, R. M., E. Bossy-Wetzel, D. R. Green, and D. D. Newmeyer. 1997. Cytochrome c activation of CPP32-like proteolysis plays a critical role in a Xenopus cell-free apoptosis system. *EMBO J.* **16:** 4639–4649.

30. Bhuyan, A. K., A. Varshney, and M. K. Mathew. 2001. Resting membrane potential as a marker of apoptosis: studies on *Xenopus* oocytes microinjected with cytochrome *c. Cell Death Differ.* **8:** 63–69.

31. Braun, T., S. Dar, D. Vorobiov, L. Lindemboim, N. Dascal, and R. Stein. 2003. Expression of Bcl-xs in Xenopus oocytes induces BH3-dependent and caspase-dependent cytochrome c release and apoptosis. *Mol. Cancer Res.* **1:** 186–194.

32. Strum, J. C., K. I. Swenson, J. E. Turner, and R. M. Bell. 1995. Ceramide triggers meiotic cell cycle progression in *Xenopus* oocytes. *J. Biol. Chem.* **270:** 13541–13547.

33. Varnold, R. L., and L. D. Smith. 1990. Protein kinase C and progesterone-induced maturation in Xenopus oocytes. *Development.* **109:** 597–604.

34. Garcia-Ruiz, C., M. Mari, A. Morales, A. Colell, E. Ardite, and J. C. Fernandez-Checa. 2000. Human placenta sphingomyelinase, an exogenous acidic pH-optimum sphingomyelinase, induces oxidative stress, glutathione depletion, and apoptosis in rat hepatocytes. *Hepatology.* **32:** 56–65.

35. Morales, A., C. García-Ruiz, M. Miranda, M. Marí, A. Colell, E. Ardite, and J. C. Fernández-Checa. 1997. Tumor necrosis factor increases hepatocellular GSH levels by transcriptional regulation of the heavy subunit chain of γ-glutamylcysteine synthetase. *J. Biol. Chem.* **272:** 30371–30380.

36. Tanaka, H., I. Matsumura, S. Ezoe, Y. Satoh, T. I. Sakamaki, C. Albanese, T. Machii, R. G. Pestell, and Y. Kanakura. 2002. E2F1 and c-Myc potentiate apoptosis through inhibition of NF-kappaB activity that facilitates MnSOD-mediated ROS elimination. *Mol. Cell.* **9:** 1017–1029.

37. Crow, J. P. 1997. Dichlorodihydrofluorescein and dihydrorhodamine 123 are sensitive indicators of peroxynitrite in vitro: implications for intracellular measurement of reactive nitrogen and oxygen species. *Nitric Oxide.* **1:** 145–157.

38. García-Ruiz, C., A. Morales, A. Colell, A. Ballesta, J. Rodes, N. Kaplowitz, and J. C. Fernández-Checa. 1994. Effect of chronic ethanol feeding on glutathione and functional integrity of mitochondria in periportal and perivenous rat hepatocytes. *J. Clin. Invest.* **94:** 193–201.

39. Blitterswijk, W. J., A. van der Luit, R. Veldman, M. Verheij, and J. Borst. 2003. Ceramide: second messenger or modulator of membrane structure and dynamics? *Biochem. J.* **369:** 199–211.

40. Fanani, M. L., S. Hartel, R. G. Oliveira, and B. Maggio. 2002. Bidirectional control of sphingomyelinase activity and surface topography in lipid monolayers. *Biophys. J.* **83:** 3416–3424.

41. Sot, J., L. A. Bagatoll, F. M. Goñi, and A. Alonso. 2006. Detergent-resistant, ceramide-enriched domains in sphingomyelin/ceramide bilayers. *Biophys. J.* **90:** 903–914.

42. Contreras, F. X., G. Basañez, A. Alonso, A. Herrmann, and F. M. Goñi. 2005. Asymmetric addition of ceramides but not dihydroceramides promotes transbilayer (flip-flop) lipid motion in membranes. *Biophys. J.* **88:** 348–359.

43. Contreras, F. X., A. V. Villar, A. Alonso, R. N. Kolesnick, and F. M. Goñi. 2003. Sphingomyelinase activity causes transbilayer lipid translocation in model and cell membranes. *J. Biol. Chem.* **278:** 37169–37174.

44. Smith, L. D. 1989. The induction of oocyte maturation: transmembrane signaling events and regulation of the cell cycle. *Development.* **107:** 685–699.

45. De Smedt, V., H. Rime, C. Jessus, and R. Ozon. 1995. Inhibition of glycosphingolipid synthesis induces p34cdc2 activation in Xenopus oocyte. *FEBS Lett.* **375:** 249–253.

46. Fernandez-Checa, J. C. 2003. Redox regulation and signaling lipids in mitochondrial apoptosis. *Biochem. Biophys. Res. Commun.* **304:** 471–479.

47. Liu, B., and Y. A. Hannun. 1997. Inhibition of neutral magnesium-dependent sphingomyelinase by glutathione. *J. Biol. Chem.* **272:** 16281–16287.

48. Ghibelli, L., C. Fanelli, G. Rotilio, E. Lafavia, S. Coppola, C. Colussi, P. Civitareale, and M. R. Ciriolo. 1998. Rescue of cells from apoptosis by inhibition of active GSH extrusion. *FASEB J.* **12:** 479–486.

49. Van den Dobbelsteen, D. J., C. S. Nobel, J. Schlegel, I. A. Cotgreave, S. Orrenius, and A. F. Slater. 1997. Rapid and specific efflux of reduced glutathione during apoptosis induced by anti-Fas/APO-1 antibody. *J. Biol. Chem.* **271:** 15420–15427.

50. Lakhani, S. A., A. Masud, K. Kuida, G. A. Porter, Jr., C. J. Booth, W. Z. Mehal, I. Inayat, and R. A. Flavell. 2006. Caspases 3 and 7: key mediators of mitochondrial events of apoptosis. *Science.* **311:** 847–851.

51. Kobrinsky, E., A. I. Spielman, S. Rosenzweig, and A. R. Marks. 1999. Ceramide triggers intracellular calcium release via the IP3 receptor in *Xenopus laevis* oocytes. *Am. J. Physiol.* **277:** C665–C672.

52. Morales, A., and J. C. Fernandez-Checa. 2007. Pharmacological modulation of sphingolipids and role in disease and cancer cell biology. *Mini Rev. Med. Chem.* **7:** 371–382.

53. Martin, S. F., F. Navarro, N. Forthoffer, P. Navas, and J. M. Villalba. 2001. Neutral magnesium-dependent sphingomyelinase from liver plasma membrane: purification and inhibition by ubiquinol. *J. Bioenerg. Biomembr.* **33:** 143–153.

54. Colell, A., O. Coll, M. Mari, J. C. Fernández-Checa, and C. Garcia-Ruiz. 2002. Divergent role of ceramide generated by exogenous sphingomyelinases on NF-kappa B activation and apoptosis in human colon HT-29 cells. *FEBS Lett.* **526:** 15–20.